

## Supporting Information

### **Efficient Li<sup>+</sup>-doping strategy to optimize the band alignment of Cu<sub>2</sub>ZnSn(S,Se)<sub>4</sub>/CdS interface by Se&LiF co-selenization process**

*Hongling Guo, <sup>a</sup> Gang Wang, <sup>b</sup> Ruitao Meng, <sup>a</sup> Yali Sun, <sup>a</sup> Siyu Wang, <sup>a</sup> Shengli Zhang, <sup>a</sup> Jianyu Wu, <sup>a</sup> Li Wu, <sup>c</sup> Guangxin Liang, <sup>d</sup> Hui Li, <sup>e</sup> and Yi Zhang<sup>\*a</sup>*

- a. Institute of Photoelectronic Thin Film Devices and Technology and Tianjin Key Laboratory of Thin Film Devices and Technology, Nankai University, Tianjin 300350, P.R. China.
- b. Changchun Institute of Applied Chemistry, Chinese Academy of Sciences, Changchun, Jilin 130022, P. R. China.
- c. Key Laboratory of Weak-Light Nonlinear Photonics, Ministry of Education, School of Physics, Nankai University, Tianjin 300071, P. R. China
- d. College of Physics and Optoelectronic Engineering, Shenzhen University, Shenzhen 518060, P. R. China
- e. Institute of Electrical Engineering, Chinese Academy of Science, Beijing 100190, P. R. China

#### Corresponding Author

Yi Zhang, E-mail: [yizhang@nankai.edu.cn](mailto:yizhang@nankai.edu.cn)

#### Defect level calculation

The defect level ( $E_A$ ) and the defect desitity ( $N_t$ ) can be estimated from the admittance results for device W/O and W/, respectively. The deep defects charge and discharge speed is slow, and they can contribute to the capacitance signal at high temperature and low frequency. However, under low temperature and high frequency test conditions, the deep defects will be frozen and unable to respond to capacitance signal. According to the dependence of capacitance signal and temperature,  $E_A$  and  $N_t$  can be extracted from the following equations.

$$\omega_0 = 2\xi_0 T^2 \exp\left(\frac{-E_A}{KT}\right) \quad (1)$$

$$E_\omega = kT \ln\left(\frac{2\beta_p N_v}{\omega}\right) \quad (2)$$

$$N_t(E_\omega) = -\frac{U_d}{qW_d} \cdot \frac{dC}{d\omega} \cdot \frac{\omega}{kT} \quad (3)$$

where  $\omega_0$  is the inflection point frequency. For each  $C(f)$  curve,  $\omega_0$  is the maxima of  $\omega \cdot dC/d\omega$  vs  $\omega$  plot,  $\xi_0$  is a temperature-independent thermal emission prefactor.  $\beta_p$  is the capture coefficient,  $N_v$  is the effective density of states in the valance band.  $\omega$  is frequency,  $E_\omega$  is the defect energy on the top of valence band maximum (VBM).  $U_d$  is the built-in voltage in the junction,  $W_d$  is the depletion region width, and  $k$  is the Boltzmann constant.

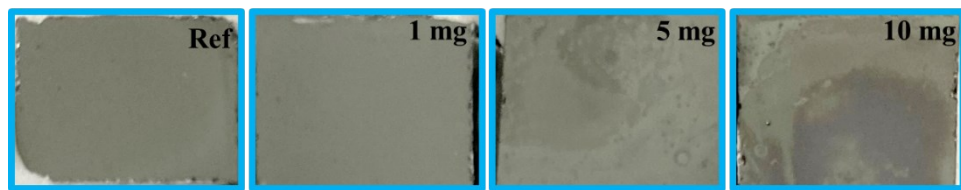


**Fig. S1** Digital photographs of CZTSSe absorber films co-selenized at 570 °C for 20 min with LiF: 0 mg (Ref), 1 mg, 5 mg, 10 mg.

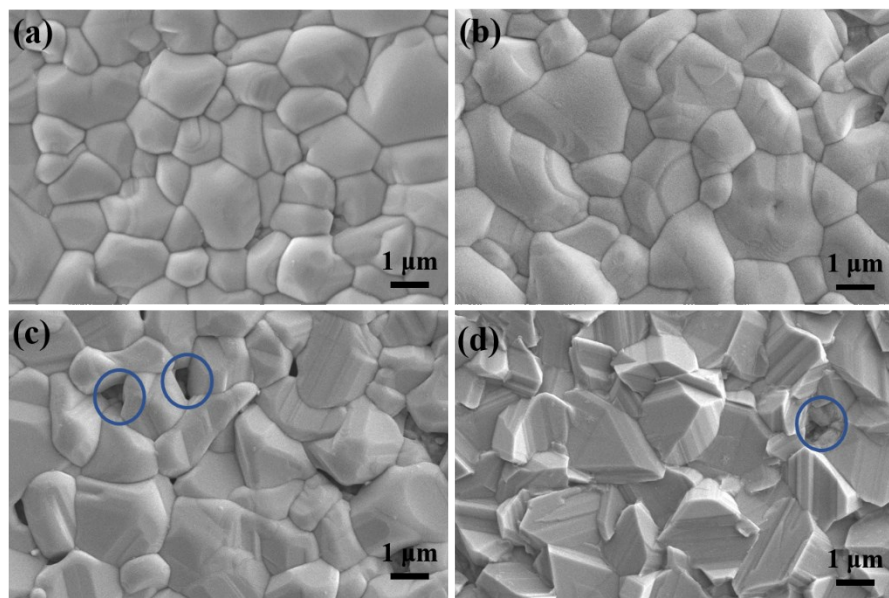


**Fig. S2** (a-d) Top-view SEM images of CZTSSe absorber films co-selenized at 570 °C for 20 min with LiF: 0 mg (Ref), 1 mg, 5 mg, 10 mg.

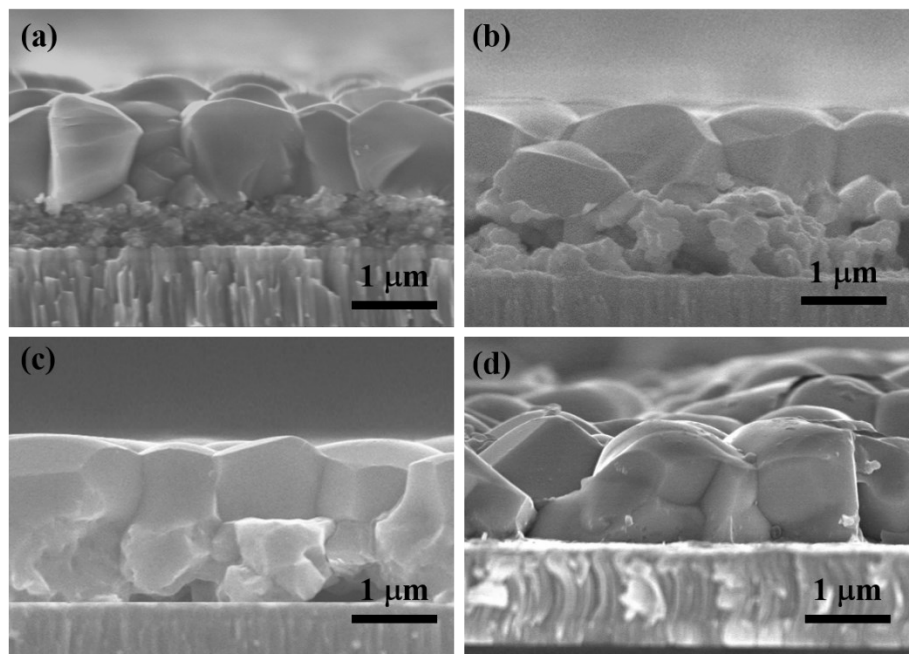


**Fig. S3** (a-d) Cross-sectional SEM images of CZTSSe absorber films co-selenized for 20 min while adding 1 mg of LiF at different annealing temperatures: 480 °C, 510 °C, 550 °C, 570 °C.

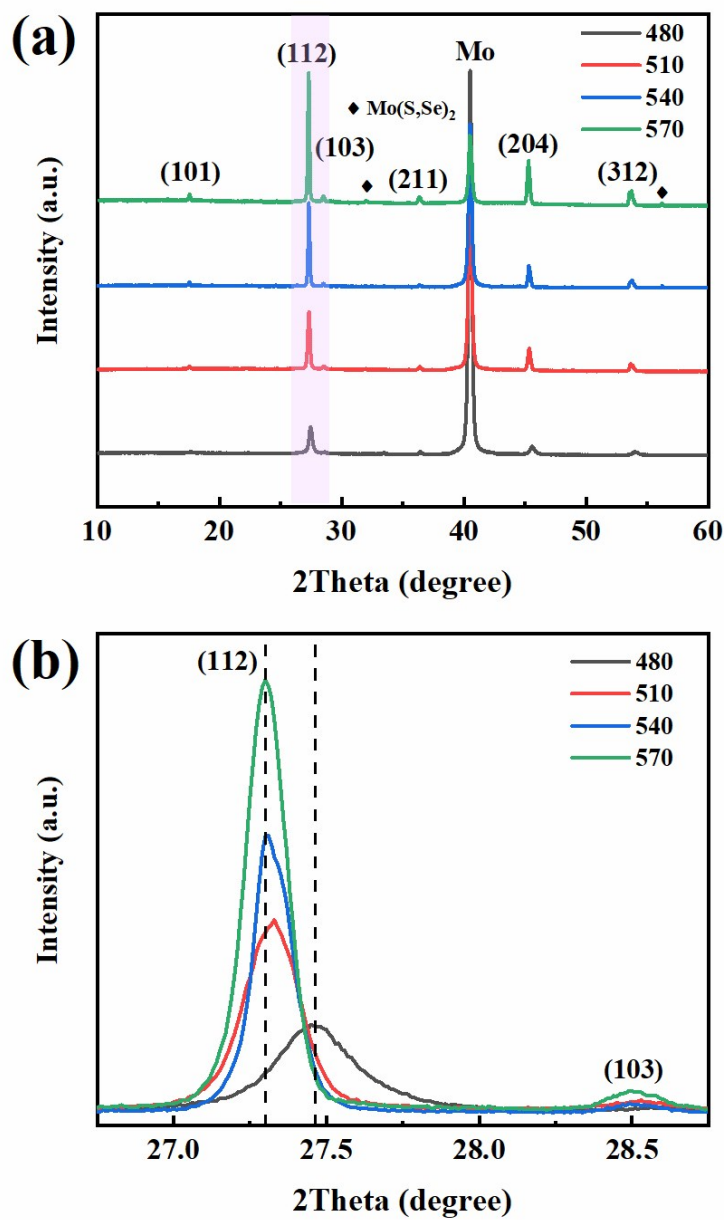


**Fig. S4** (a) XRD patterns of CZTSSe absorber films co-selenized for 20 min while adding 1 mg of LiF with LiF at 480 °C, 510 °C, 540 °C, 570 °C. (b) The (112) diffraction peaks for all the samples are enlarged to show peak shift.

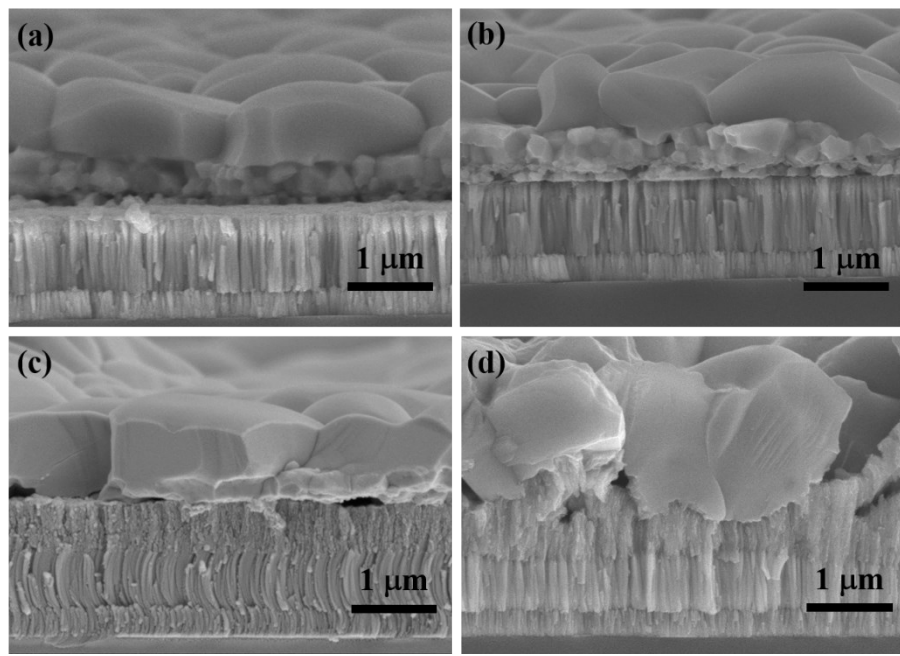


**Fig. S5** (a-d) Cross-sectional SEM images of CZTSSe absorber films co-selenized at 570 °C while adding 1 mg of LiF at different annealing time: 10 min, 15 min, 20 min, 25 min.

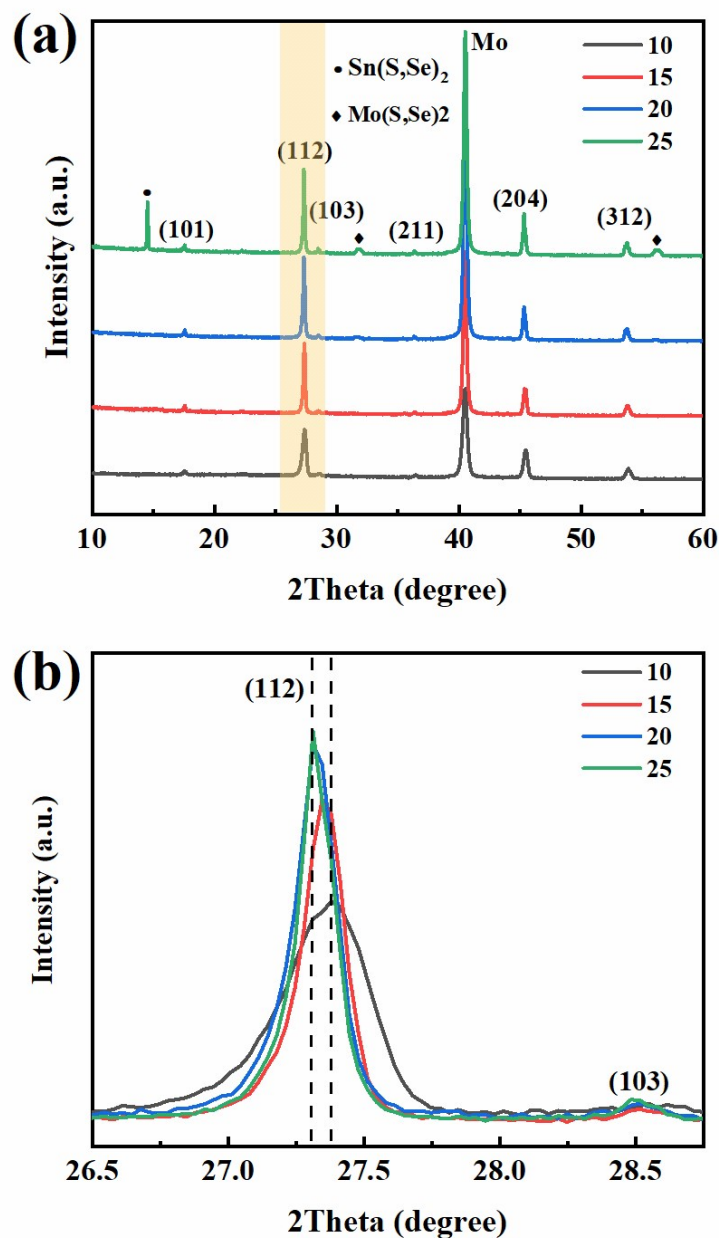


**Fig. S6** (a) XRD patterns of CZTSSe absorber films co-selenized at 570 °C while adding 1 mg of LiF at different annealing time with LiF at 10 min, 15 min, 20 min, 25 min. (b) The (112) diffraction peaks for all the samples are enlarged to show peak shift.

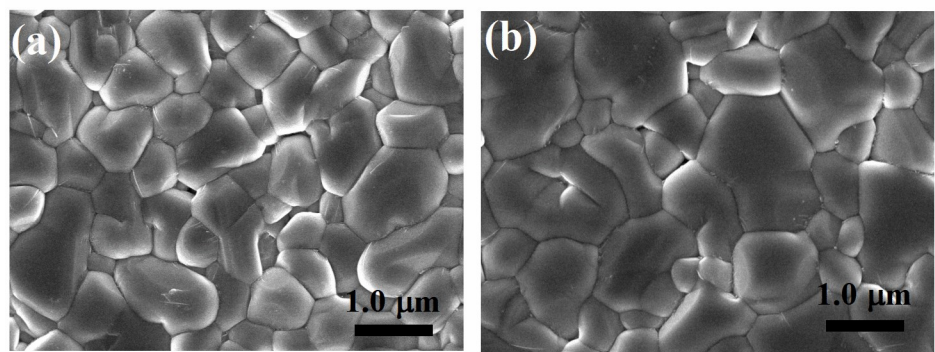


**Fig. S7** Top-view SEM images of samples W/O and W/, respectively.

**Table S1** Elemental composition ratios of sample W/O and W/. Results were obtained from top-view EDX measurements.

Sample	Cu/(Zn+Sn)	Zn/Sn	Se/(S+Se)
W/O	0.792	1.11	0.917
W/	0.758	1.07	0.928

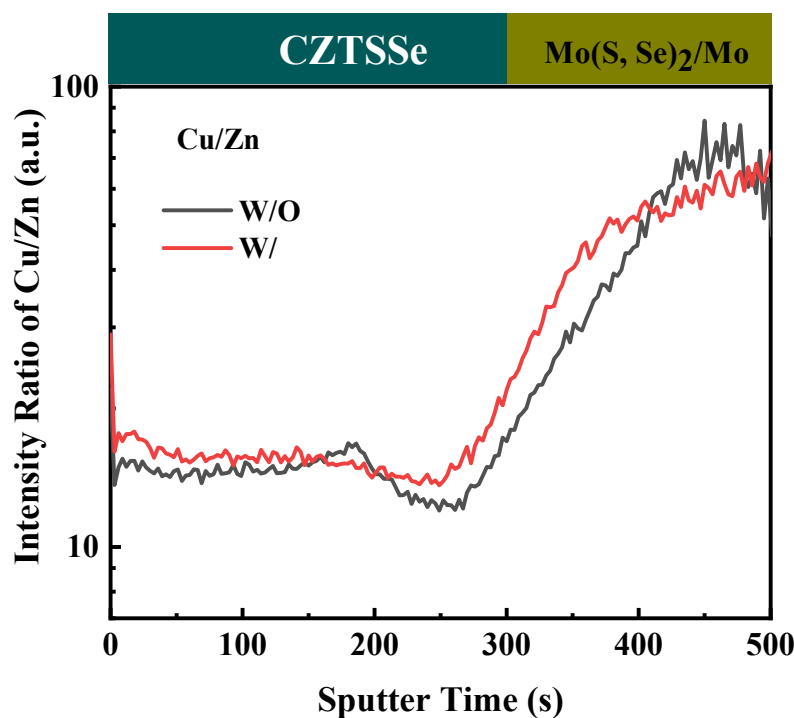


**Fig. S8** Intensity ratios of Cu/Zn for samples W/O and W/, respectively.

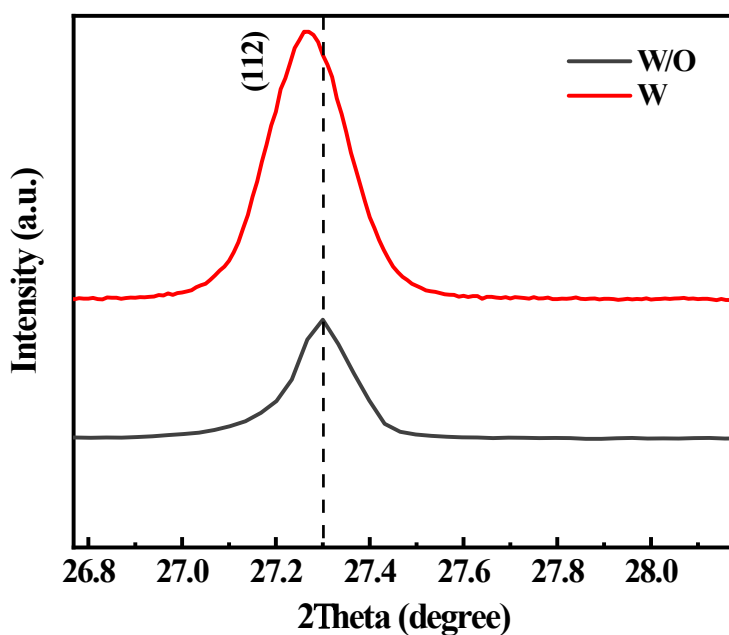


**Fig. S9** The enlarged view (112) peaks of samples W/O and W/, respectively.

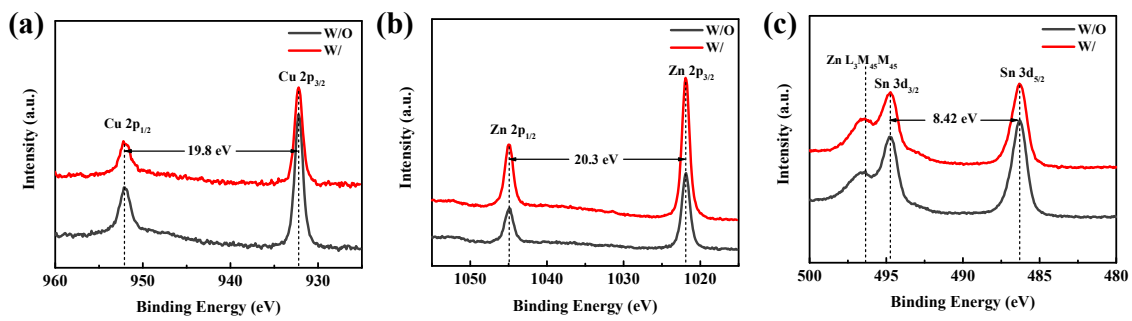


**Fig. S10** (a-c) High-resolution XPS spectra of the Cu 2p, Zn 2p, Sn 3d core level of samples W/O and W/. The Zn L<sub>3</sub>M<sub>45</sub>M<sub>45</sub> Auger peak at 496.3 eV can be observed on the left side of the Sn 3d core level spectrum.

**Table S3** Photovoltaic performance and Voc deficit for CZTSSe-based solar cells.  $x$ : unkown

	$V_{OC}$ (V)	$E_g$ (eV)	$V_{OC}$ -deficit (V)	$\eta$ (%)	Li <sup>+</sup> -doping strategy	Ref
CZTSSe	0.531	1.13	0.599	11.6		1
CZTSSe	0.496	1.11	0.614	11.5		2
CZTSSe	0.449	1.04	0.591	11.8		3
CZTSSe	0.459	1.23	0.771	6	precursor-doping	4
CZTSSe	0.408	1.04-1.09	<sup>a</sup> $\geq 0.632$	6.7		5
CZTSSe	0.380	1.08	0.7	6		6
CZTSSe	0.398	$x$	<sup>b</sup> $\geq 0.602$	5.21	soaking	7
CZTSSe	0.477	1.06	0.583	11.63	co-selenization	This work

<sup>a</sup> The minimum  $V_{OC}$ -deficit was calculated based on the minimum band gap of 1.04 eV mentioned in the literature.

<sup>b</sup> The minimum  $V_{OC}$ -deficit was calculated assuming  $x = 1.0$  eV.

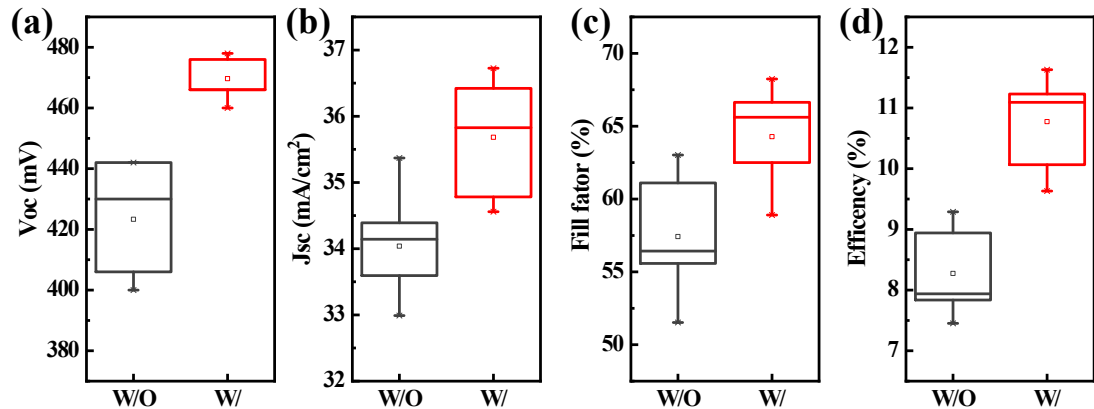


**Fig. S11** (a-d) The statistic photovoltaic performances of the Voc, Jsc, Fill factor and efficiencies of the devices W/O and W/.

**Table S4** Statistics of CZTSSe solar cell parameters for 18 cells for devices W/O and W/.

	$V_{OC}$ (V)		$J_{SC}$ (mA/cm <sup>2</sup> )		FF (%)		$\eta$ (%)	
	W/O	W/	W/O	W/	W/O	W/	W/O	W/
Cell #1	0.4	0.46	34.61	36.73	57.14	58.9	7.91	9.95
Cell #2	0.406	0.478	34.29	36.6	55.79	63.47	7.77	11.1
Cell #3	0.412	0.466	34.14	34.56	56.43	62.51	7.94	10.07
Cell #4	0.43	0.476	35.37	36.42	51.52	66.64	7.84	11.54
Cell #5	0.442	0.477	34.39	36.34	61.11	67.09	9.29	11.63
Cell #6	0.442	0.472	33.59	35.83	55.58	65.61	8.25	11.09
Cell #7	0.442	0.466	33.15	34.58	61.93	66.62	9.07	10.74
Cell #8	0.43	0.466	32.99	34.78	63.03	59.43	8.94	9.63
Cell #9	0.406	0.466	33.81	35.32	54.29	68.24	7.45	11.23

## References

1. A. Cabas-Vidani, S. G. Haass, C. Andres, R. Caballero, R. Figi, C. Schreiner, J. A. Márquez, C. Hages, T. Unold, D. Bleiner, A. N. Tiwari and Y. E. Romanyuk, *Adv. Energy Mater.*, 2018, **8**.
2. S. G. Haass, C. Andres, R. Figi, C. Schreiner, M. Bürki, Y. E. Romanyuk and A. N. Tiwari, *Adv. Energy Mater.*, 2018, **8**.
3. H. Xin, S. M. Vorpahl, A. D. Collord, I. L. Braly, A. R. Uhl, B. W. Krueger, D. S. Ginger and H. W. Hillhouse, *Phys. Chem. Chem. Phys.*, 2015, **17**, 23859-23866.
4. Y. Yang, X. Kang, L. Huang and D. Pan, *ACS Appl. Mater. Interfaces*, 2016, **8**, 5308-5313.
5. Y. Yang, L. Huang and D. Pan, *ACS Appl. Mater. Interfaces*, 2017, **9**, 23878-23883.
6. Y.-T. Hsieh, Q. Han, C. Jiang, T.-B. Song, H. Chen, L. Meng, H. Zhou and Y. Yang, *Adv. Energy Mater.*, 2016, **6**.
7. G. Altamura, M. Wang and K.-L. Choy, *Sci. Rep.*, 2016, **6**.